

Experimental demonstration of the water-holding property of three-dimensional vortices

T. TÉL^{1,2,3}, L. KADI^{1,4}, I. M. JÁNOSI^{1,5} and M. VINCZE^{1,2}

¹ von Kármán Laboratory for Environmental Flows, Eötvös University - Pázmány Péter s. 1/A, H-1117 Budapest, Hungary

² MTA-ELTE Theoretical Physics Research Group - Pázmány Péter s. 1/A, H-1117 Budapest, Hungary

³ Institute for Theoretical Physics, Eötvös University - Pázmány Péter s. 1/A, H-1117 Budapest, Hungary

⁴ Ecole Polytechnique Fédérale de Lausanne - Route Cantonale, 1015 Lausanne, Switzerland

⁵ Department for the Physics of Complex systems, Eötvös University - Pázmány Péter s. 1/A, H-1117 Budapest, Hungary

received 26 April 2018; accepted in final form 20 August 2018

published online 17 September 2018

PACS 47.32.C- – Vortex dynamics

PACS 01.50.My – Demonstration experiments and apparatus

PACS 47.32.-y – Vortex dynamics; rotating fluids

Abstract – When injecting dye into a vertical vortex generated by a commercial magnetic stirrer, one finds that dye remains captured around the vortex core over minutes, while it gets mixed with the water outside this region rather rapidly. Thus, considering its horizontal motion, the dye becomes trapped within a critical radius, even though the vortex structure (and the dyed region) is aperiodically time-dependent due to the oscillations of the position of the stirring bar. According to a recent paper by Haller and coworkers (*J. Fluid Mech.*, **795** (2016) 136), three-dimensional time-dependent vortices should be defined as rotating, material-holding tubular regions of the fluid. We report here about a set of experiments carried out with magnetic-stirrer-generated vortices which appears to provide the first pieces of evidence supporting the theory in a very elementary set-up that is accessible even in high schools. Our data also provide information about quantities not predicted by the theory, *e.g.*, the lifetime of dye spent within the vortex. We show that the maximum radius of the stable dye cylinders, *i.e.*, the horizontal extent of the vortex, hardly depends on the rotational frequency of the stirrer bar – at least in the range investigated – but increases with the length of the bar. A generalization of this finding leads to the conclusion that the size of the material-holding region of the vortices in nature should be proportional to the size of the surface (or pressure) depression accompanying the vortex.



Copyright © EPLA, 2018

Published by the EPLA under the terms of the Creative Commons Attribution 3.0 License (CC BY). Further distribution of this work must maintain attribution to the author(s) and the published article's title, journal citation, and DOI.

Introduction. – There is a recent interest in Lagrangian Coherent Structures (LCS) [1–5] and in the application of this concept in flows ranging in size from laboratory to planetary scales (see, *e.g.*, [3,4]). In flows of arbitrary time dependence, LCS provide a skeleton of material surfaces and organize details of the tracer dynamics. Basic examples of them are material filaments or vortex cores. The formers, also called hyperbolic LCS, are the generalization of stable or unstable manifolds of chaotic sets which change in time in an aperiodic fashion, as demonstrated also in experiments [6]. Understanding the

latter, the elliptic LCS, has required different approaches. In two-dimensional flows a variational principle leads to an analogy with the black holes of astrophysics based on strict mathematical arguments (see, *e.g.*, [7]). These variational approaches did, however, determine only the edge of the vortex, and did not provide any hint on their internal structure.

There are several coexisting definitions of vortices [8] even in the stationary case, based on Eulerian properties like vorticity. In non-stationary cases the Eulerian and Lagrangian views are known to differ and the authors of [9]

suggest a Lagrangian definition. The definition used in [9] is based on the integral along trajectories of fluid elements of the difference of the vorticity from its spatial mean. This quantity is the so-called Lagrangian Averaged Vorticity Difference, LAVD. A LAVD surface corresponds to a material surface of equal rotation relative to the mean rotation of the deforming fluid volume. The *outermost closed* surface of LAVD is defined as the boundary of a vortex, and the internal structure is predicted to be a set of concentric tubular surfaces.

In an experiment it is practically impossible to measure LAVD values (based on the entire high-resolution spatio-temporal knowledge of the 3D velocity field), in our investigations we therefore consider the boundary of a vortex to be the outermost closed material surface. It is worth mentioning that the presence of a similarly coherent separation barrier between internal and external flow regions has long been known in the context of point vortex advection [10,11]: for point vortices of general time dependence there is a disk moving with each of them where passive particles cannot enter from outside, and within which particles remain trapped forever [12–14]. The finite size of these vortex cores is in sharp contrast with the vanishing size of the region where vorticity is concentrated. This is in harmony with the view of [9] according to which a vortex should be defined via its Lagrangian properties instead of vorticity. It is perhaps due to the two-dimensional and rather singular character ($v \sim 1/r$) of point vortices that this dichotomy was not realized in its full depth by the community in the past decades and did not call for a general definition of vortices.

Our aim here is to demonstrate the water-holding property of a generally time-dependent three-dimensional vortex realized in a rather elementary set-up utilizing magnetic stirrers.

Commercial magnetic stirrers are commonly used to dissolve materials in fluids. The main component of the device is a magnet rotating at an adjustable frequency around a fixed vertical axis *below* a flat horizontal cover. The rotating magnetic field of the magnet brings a magnetic stirrer bar, whose axis of rotation is not fixed, into rotation on the bottom of a tank placed onto the horizontal cover. If the tank is filled with a liquid the bar generates fluid motion, which is believed to yield efficient stirring and mixing. The typical pattern of such flows is a pronounced vortex above the stirrer bar [15,16] accompanied with a depression of the free surface, the funnel. The qualitative characterisation of the flow in the setup can be used to better understand the efficiency/inefficiency of the stirrer, and related applications [17–23]. The tangential velocity far away from the center has been measured to be proportional to $1/r$ [15]. Due to the lack of reliable velocity measurements¹ in the center, one can only speculate

¹It is to be noted that although the widespread particle image velocimetry (PIV) technique – the correlation-based feature tracking of tracer particles within a quasi-2D laser plane in the fluid – seems to be a relatively straightforward way to obtain velocity fields

that there is a central region exhibiting rigid body rotation ($v \sim r$) but it remains unknown where the crossover between this domain and the $v \sim 1/r$ region lies. Note that even if the entire instantaneous velocity field was known, this *per se* would not provide direct information on Lagrangian properties [24] (like water-holding) in that given time instant.

In order to understand mixing properties, one should study Lagrangian features best monitored by the injection of dye. When injecting dye into a vortex, generated by a magnetic stirrer, one finds a surprising phenomenon: the dye remains captured around the vortex core over minutes, while it becomes mixed with the water outside this region rather rapidly. It is worth noting that this phenomenon was already observed and briefly mentioned in earlier papers but without any interpretation [15]. Reference [16] concentrated on a related phenomenon, on the capturing of light finite-size particles by the center of the vortex. It was pointed out that the particle motion is then nothing but the fingerprint of a noisy chaotic attractor in the fluid that can be observed by naked eye. The authors of [25] studied a fast flow through a cone-shaped nozzle. When injecting ink into the nozzle, they observed with surprise that an initially turbid phase cleaned out and led to the appearance of a long-lasting dye cylinder whose diameter was about that of the smaller hole of the nozzle. In contrast to the magnetic-stirrer-generated vortex, this dye cylinder is hollow due to the strong plughole-like [23,26] flow through the nozzle.

The appearance of the theory of [9] provides an appropriate framework for the interpretation of such findings. In this spirit, we carried out a series of experiments with the aim of demonstrating that magnetic-stirrer-generated vortices keep the dye captured in a finite cylindrical domain, and provide examples of 3-dimensional elliptic LCS. Our aim was also to find out which quantities influence the properties of such time-dependent Lagrangian vortices which do not follow from the theory of [9], like, *e.g.*, the lifetime of dye spent in the vortex, its fine structure, transient phenomena, and the average width of the vortex.

Experimental setup. – Figure 1 shows the basic setup with a cylindrical container of radius $R = 22.3$ cm, filled with tap water at room temperature up to the height of $H = 22$ cm, and put on top of the magnetic stirrer. The horizontal scale of the apparatus suggests that the boundary effects originating from the vertical walls are negligible in the central region, thus the properties observed approximate those of vortices in an unbounded domain. The stirrer (white horizontal bar with two black markers at its

at a first glance, carrying out such measurements in the central region of the vortex, however, turns out to be extremely difficult to realize in practice. The image of this inner domain (viewed from above) is highly distorted by the optical refraction by the funnel, moreover, the strong perpendicular flow in any relevant plane makes it practically impossible to obtain reliable velocity fields with current technologies.

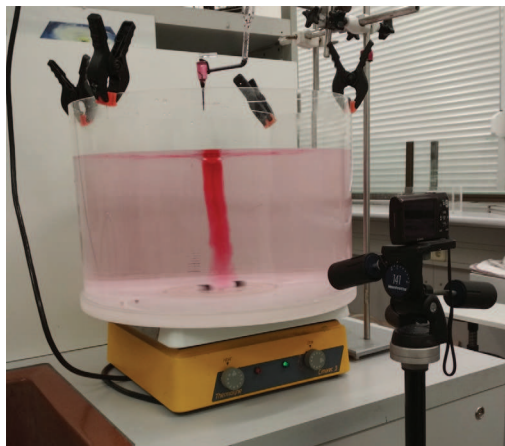


Fig. 1: (Color online) The experimental setup with the video camera on the right.

Table 1: Length and width of the stirrer bars used in the experiments

Stirrer bar	Length a (cm)	Width c (cm)
1	8	1.1
2	5	1.1
3	4.1	0.9

end) is subjected to friction on the plastic bottom of the container. The narrow nozzle above the midpoint of the container was tailored to let a given volume of food dye (practically a passive tracer) fall, in the form of droplets, onto the surface of the liquid. For subsurface injection we used syringes.

The most striking feature is the red columnar structure in the middle, just above the stirrer bar, clearly separated from the rest of the fluid which is practically transparent. Measurements are carried out with three different stirrer bars the dimensions of which are summarized in table 1. Regarding the video analyses, fig. 2 shows the typical sharp and narrow tubular pattern, the lowest part of which overlaps with the region where the rod rotates. Our measurements concentrate on an intermediate region, marked by a black rectangle, where the width of the dye cylinder is approximately constant. It is in this region where we measure the location and width of the cylinder, and within which we determine the average lifetime τ of the dye within the vortex.

τ was measured by dropping a certain volume (0.4 ml) in the middle of the funnel and counting the number of “dark red” pixels within the black rectangle of fig. 2. To determine which pixels are “dark red”, we set filters for RGB values and each pixel of each frame is passed through these filters. Only the pixels which pass the filter are counted. The filtering values are subjective, but since the criteria is the same for all frames and pixels, our results can be compared between frames. The lifetime is finite because the downwelling dye reaches the bottom of the

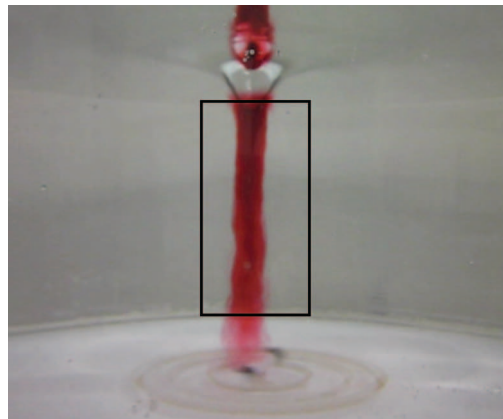


Fig. 2: (Color online) A typical frame from a video record with the region, black rectangle, from which experimental data are taken.

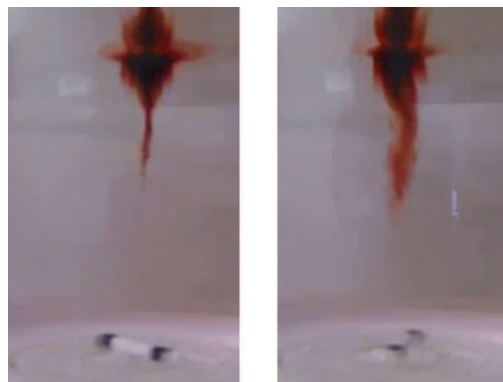


Fig. 3: (Color online) Initial stages of the development of a dye cylinder.

container where the stirrer bar rotates and where strong mixing takes place in a shallow region whose height is proportional to the width c of the stirrer bars (about 10 mm, see table 1).

The frequency range scanned was limited by two factors, both due to our apparatus: first, all stirrer bars have a maximum rotational frequency at which they undergo a mechanical instability, and get ejected from the center upon which stirring practically stops. Second, the minimal rotational frequency is given by the lowest level on the magnetic stirrer. At this lowest level of energy input, the longest bar rotates with the smallest frequency since the frictional torque on the button is largest for this bar. Thus, both minimal and maximal frequencies depend on the stirrer bar used.

Qualitative observations. – It is interesting to observe the initial dynamics of a droplet placed on the free surface of the water body close to the middle of the vortex before a quasi-stationary dye cylinder is built up. One often sees, as fig. 3 illustrates, that the sinking is not uniform, the innermost region is the fastest sinking one in the form of a “worm” of gradually increasing length.

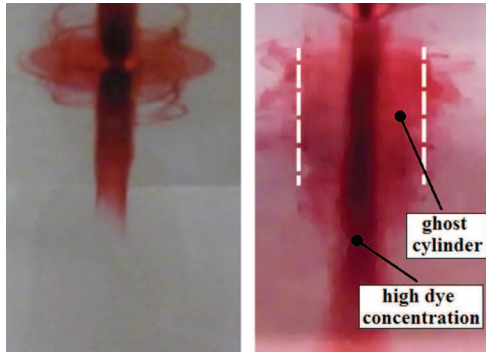


Fig. 4: (Color online) Left panel: a transient “collar”. Right panel: a “ghost cylinder” about the vortex tube of high dye concentration.



Fig. 5: (Color online) Left and right panels: side and top view of a dye cylinder exhibiting fine structures. Note the red tongue in the lower part of the dyed region in the right panel, which quickly disappears.

If a certain amount of dye is injected in a region outside a critical radius measured from the center, it does not sink rapidly, rather it becomes distributed along an irregular pattern, the “collar” in the upper region of the flow (see fig. 4, left panel), but, after some time, this amount of dye becomes fully diluted, and hardly visible. The collar is qualitatively similar to the non-closed LAVD surfaces determined in the simulation of an oceanographic vortex in fig. 13(a) of [9]. It might also happen that some dye off the critical radius penetrates the bulk of the flow and forms a “ghost cylinder” outside the cylinder of high dye concentration (see fig. 4, right panel) but this also vanishes after some time, much before the typical lifetime (minutes) of the high concentration cylinder.

Figure 5 shows a simultaneous side and top view of a stationary dye cylinder. In the left panel one sees that the dye cylinder is not homogeneous, rather it appears to consist of a set of concentric cylinders. This is consistent with the observation of [9] according to which there are material-holding tubular surfaces within the vortex. It is the obviously inhomogeneous injection of dye which might lead to higher or lower concentrations between the

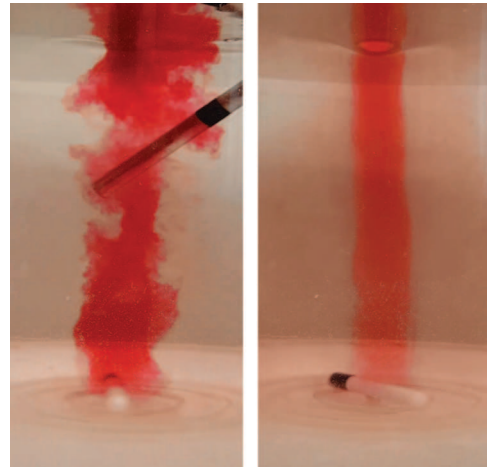


Fig. 6: (Color online) Left panel: destructed pattern appearing right after cutting the dye cylinder through with a metal rod. Right panel: the spontaneously reconstructed dye cylinder about 10 seconds after the removal of the rod.

concentric cylindrical surfaces. In the top view (right panel) we see that there is a tongue along the perimeter of the core but it decays away in time as further observation (not shown) indicates. This is in accordance with the finding of the theory according to which a vortex experiences only tangential material filamentation. Both features are summarized schematically in fig. 2 of [9], and are in full harmony with the topology of the polar vortex (determined in [27] by a variational approach) and with our own observations.

To test the stability of the dye cylinder, we injected, at a low stirring frequency, a certain amount of dye into the central region and let the dye cylinder develop. After some time, however, we started to increase the frequency gradually with a finite speed, and reached an increase of a factor of about 3 in half a minute. The cylinder did not become destroyed (not shown), moreover, it survived even the return to the original stirring frequency. It is worth mentioning that the width of the cylinder became markedly smaller at the highest frequency, while stationary measurements (see later) indicate practically no change of the width. This is in harmony with a typical feature of experiments with ramped systems [28] according to which instantaneous properties on the ramp often differ from those observed at the same parameter kept constant in time.

The robustness of the dye cylinder can be tested by immersing a rod into the fluid and approaching it towards the cylinder. One observes that even before the rod touches the outermost closed dye surface, it becomes destructed and an originally inner surface becomes the new outermost one. A complete destruction takes place when the pattern is cut through with the rod (fig. 6, left panel). Surprisingly enough, however, after the removal of the rod, the original cylinder is recovered, even if in a much more pale form since most of the dye escaped the central region due to the very strong perturbation. The water-holding property

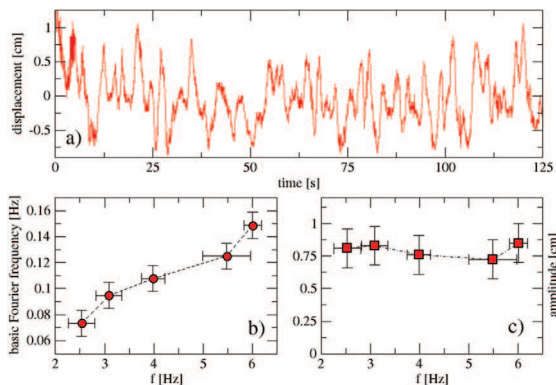


Fig. 7: (Color online) (a) A typical time series of the position of a dye cylinder with the same stirrer as in fig. 1. (b) Dependence of the basic Fourier frequency and (c) the amplitude of oscillations on the frequency f of the stirrer.

is thus rather robust and recovers itself once the original flow is re-established.

The qualitative observations listed here illustrate clearly the basic Lagrangian properties of vortices. The used set-up based on a magnetic stirrer and a cylindrical container is relatively inexpensive, easy to run, therefore, this type of experiment is ideally suited for the demonstration of the recently emerged view on time-dependent vortices to school kids or university students. The sharp boundary of the dyed region resembles that of the domain carrying debris, sand and water in tornadoes [29], dust devils [30] and waterspouts [31], respectively. These observations of outermost material-holding surfaces in the laboratory and in nature reassure that the condition of [9], formulated in terms of LAVD, is well founded.

Quantitative results. – Using the aforementioned feature tracking method based on the RGB values of the sequence of frames, we can deduce the horizontal displacement of the cylinder as a function of time at a selected intermediate height. Figure 7 (a) indicates that the cylinder undergoes an oscillatory motion of relatively large amplitude (remember, the center of the stirring bar is not fixed). The dominant Fourier frequency is found to increase with the frequency of rotation, but the amplitude appears to be practically constant (panels (b) and (c) of fig. 7, respectively). The error bars along the frequency axis represent the uncertainty originating from the fact that the control button of the commercial magnetic stirrer contains levels (from 1 to 10) and these positions do not correspond to sharp frequency values, rather to intervals. The frequencies of the stirrer bars f were determined by means of a stroboscope shedding light on the stirrer bar in a periodic fashion as in [15]. The results shown in fig. 7 are obtained with the longest bar at disposal since the lifetime of the dye cylinder is too short for a precise extraction of the dominant frequency with shorter bars. Vertical error bars in panels (b) and (c) represent the full width at half-maximum of the dominant frequency peaks in the

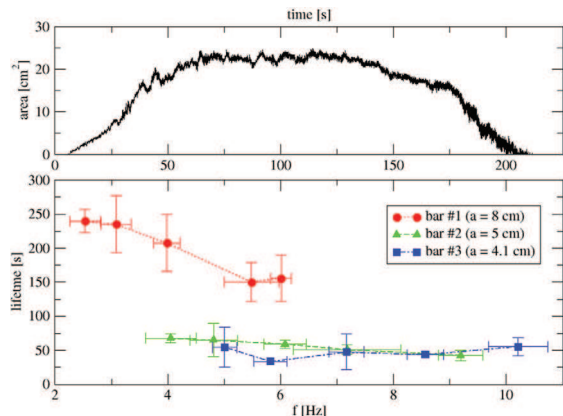


Fig. 8: (Color online) Upper panel: a typical time series of the number of “dark red” pixels as a function of time. Lower panel: average lifetime as a function of frequency f with different stirrers. Vertical error bars represent the standard deviations of the data at a given frequency.

spectra and the standard deviation of the measured data, respectively.

A typical time series of the number of “dark red pixels” within the rectangular area marked in fig. 2 is shown in the upper panel of fig. 8. The increase at the beginning is due to the downward motion of dye, starting right after dropping in took place, within the vortex, and the decrease at the end is a sign of all dye becoming washed out. We therefore considered the lifetime τ defined by the length of the “plateaued region” whose length was determined by using a threshold value. The results obtained by averaging over 3 trials for each frequency and stirrer bar are displayed in the lower panel.

For the small bars there is practically no dependence on the frequency, while the lifetime function with the longest bar appears to start with a plateau which is followed by a decrease. Observe that the lifetime on this plateau is about 5 times as large as with the other bars. This is why we carried out the Fourier analysis of fig. 7 with the longest bar only.

We also measured the position of the tip of the transient “worms” shown in fig. 3 with different stirrer bars in a few cases. The left panel (a) of fig. 9 indicates a rather disordered set of patterns in the tracks with apparent vertical fluctuations superimposed on the downward motion that seem to be coupled to the irregular horizontal oscillations of the vortex demonstrated in fig. 7. The effect of these fluctuations is reflected also in the velocity *vs.* frequency diagram of panel (b). Considering points belonging to a given bar (given color in the right panel), one is hardly able to extract any simple functional form, but considering the full set of points suggests that the average sinking velocity v of the innermost “worm” fulfills the relation $v \propto f$.

In order to determine the width d of the dye cylinders, we injected dye into a region broader than the anticipated

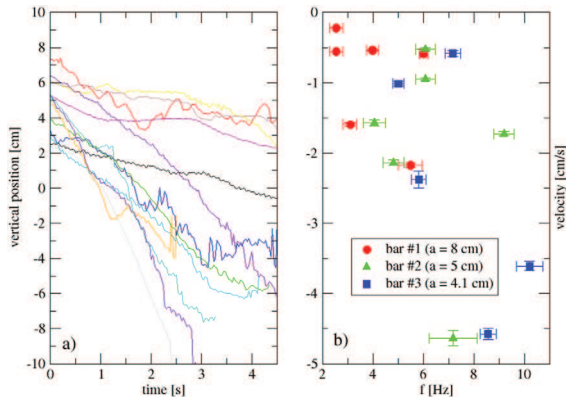


Fig. 9: (Color online) Examples of time series of the vertical coordinate of the tip of the dyed region (a) and average tip velocities (b) for different frequencies f and stirrer bars. These average velocities were obtained via linear fits to time series like the ones shown in panel (a). The vertical error bars represent the fit error (standard deviation).

width. After the “collar” and the “ghost cylinders” disappeared, considerable local variance remained and the measurement could be carried out only by naked-eye observation of the video records. We determined the width at different heights along the dye cylinder, and at different times (long before the cylinder disappeared) with any available frequency and stirrer bar, and by taking an average. The width is in principle the diameter of the outermost closed material surface. A surface of slightly larger diameter becomes, however, disrupted rather slowly, and might disappear after our measurement is over. We argue therefore that the relatively large error bars indicated for d are consequences of the inherent variability of material-holding vortices. Figure 10 summarizes all our width measurements with the three different bars used. We find practically no tendency with the frequency, but one sees a characteristic increase with the length a of the bar.

When trying to find a correlation of the average vortex width d with other quantities, the length a of the stirrer bar is a natural candidate since strong shear builds up in the flow within a cylinder of approximate diameter a . The viscous length scale $\sqrt{\nu/f}$ estimated with the smallest frequency $f \approx 2$ Hz is on the order of mm’s, much smaller than d , therefore, viscosity is not expected to play a major role in the formation of the observed coherent dye pattern. A simple argument can then be found for the frequency independence of d : Assuming the bars of identical width, and boundary effects to be negligible, the only two remaining length scales are a and g/f^2 with g as the gravitational acceleration. Any size related to the flow can then only depend on these parameters. For quantities which can be assumed to be not sensitive to gravity, the only choice is being proportional to the length of the stirrer bar. The width of the dye cylinders appears to behave like this².

²Other features of the flow, *e.g.*, the funnel-like shape of the free surface (a consequence of the pressure minimum and approximate hydrostatic balance) is related to gravity and the funnel depth is

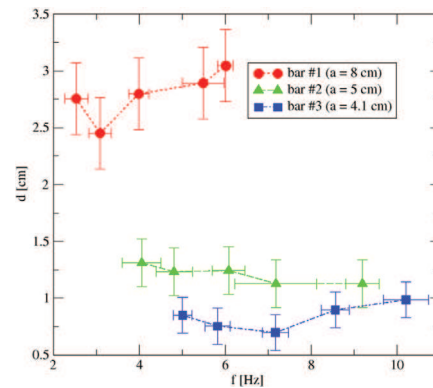


Fig. 10: (Color online) The measured average width d of dye cylinders as a function of frequency f with different stirrers.

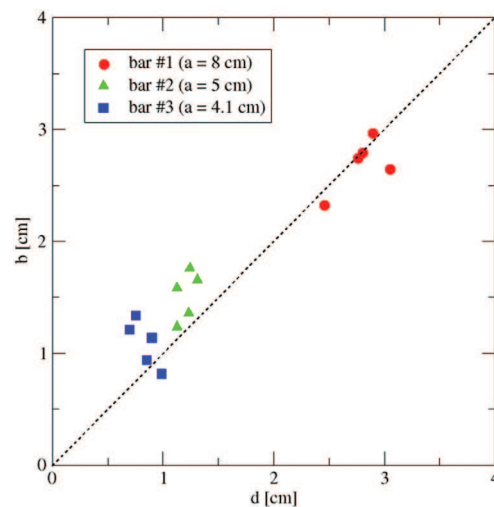


Fig. 11: (Color online) Cross-correlation between the dye cylinder and funnel widths (d and b). The dotted straight line marks the diagonal.

Vortices occurring in Nature are, however, not generated by stirrer bars. It is therefore natural to search for fluid dynamical length scales which correlate well with the width. We found that it is the width of the funnel on the free surface which correlates the best. We determined the average funnel width b (taken at the middle between the free surface and the funnel’s lowest point) with different bars and different frequencies from the video records, and found that the width b is also practically independent of f . Figure 11 displays the function b vs. d . The diagonal clearly fits very well to the data, suggesting the relation $d \approx b$.

Discussion and outlook. – The observations found can be summarized in traditional fluid dynamic terms as follows. In a reference frame comoving with the center of the vortex (such a frame is generally hard to find) the flow within the vortex is *laminar*. The very middle of it is indeed proportional to f^2 , as reported in [15].

in solid body rotation but laminar region extends further out. The boundary of the vortex is set by a local shear instability. The regular dye pattern and its long lifetime is due to the lack of turbulent fluctuations within the vortex.

In large-scale vortices in Nature viscosity is negligible [32], similarly to our experiment. Thus, the above argument of $d \approx b$ is expected to hold there as well. Our main non-trivial conclusion is that such three-dimensional vortices hold material in a *Lagrangian* tubular structure whose radius should be proportional to the size of the (pressure or surface) depression accompanying the vortex, an *Eulerian* quantity. In the particular case of planetary-scale geophysical flows the horizontal size of vortices of general time dependence is set by the Rossby radius of deformation (which might also contain stratification effects), a quantity expressing the relevance of the Coriolis force on these scales [32]. Thus, our results may imply that the domain in which water parcels are transported by oceanic eddies is approximately of the size of the local Rossby radius.

* * *

We are thankful for numerous discussions with G. HALLER during different phases of this work. We also benefited from useful comments by G. GYÖRGYI, B. KASZÁS, S. KATZ, and J. VANYÓ. We are grateful to the Erwin Schrödinger Institute, Vienna, and for its program “Mathematical aspects of physical oceanography” during which the manuscript was completed. TT also acknowledges the support of the Alexander von Humboldt Foundation. This work was also supported by the Hungarian National Research, Development and Innovation Office (NKFIH) under grants K125171 and FK125024 and by the Content Pedagogy Research Program of the Hungarian Academy of Sciences.

REFERENCES

- [1] HALLER G. and YUAN G., *Physica D*, **147** (2000) 352.
- [2] PEACOCK T. and DABIRI J., *Chaos*, **20** (2010) 017501.
- [3] PEACOCK T. and HALLER G., *Phys. Today*, **66**, issue No. 2 (2013) 41.
- [4] HALLER G., *Annu. Rev. Fluid Mech.*, **47** (2015) 137.
- [5] HADJIGHASEM A. *et al.*, *Chaos*, **27** (2017) 053104.
- [6] VOITH G. A., HALLER H. and GOLLUB J. P., *Phys. Rev. Lett.*, **88** (2002) 254501.
- [7] HALLER G. and BERON-VERA F. J., *J. Fluid Mech.*, **731** (2013) R4.
- [8] GREEN S. I. (Editor), *Fluid Vortices* (Springer, New York) 1995.
- [9] HALLER G., HADJIGHASEM A., FARAZMAND M. and HUHN F., *J. Fluid Mech.*, **795** (2016) 136.
- [10] AREF H., KADTKE J. B., ZAWADZKI I., CAMPBELL L. J. and ECKHARDT B., *Fluid Dyn. Res.*, **3** (1988) 63.
- [11] NEWTON P. K., *The N-Vortex Problem: Analytical Techniques* (Springer, New York) 2001.
- [12] NEUFELD Z. and TEL T., *Phys. Rev. E*, **57** (1998) 2832.
- [13] KUZNETSOV L. and ZASLAVSKY G. M., *Phys. Rev. E*, **61** (2000) 3777.
- [14] KUZNETSOV L. and ZASLAVSKY G. M., *Phys. Rev. E*, **58** (1998) 7330.
- [15] HALASZ G., GYURE B., JANOSI I. M., SZABO K. G. and TEL T., *Am. J. Phys.*, **75** (2007) 1092.
- [16] VANYO J., VINCZE M., JANOSI I. M. and TEL T., *Phys. Rev. E*, **90** (2014) 013002.
- [17] GIANNELLI L., SCOMA A. and TORZILLO G., *Biotechnol. Bioeng.*, **104** (2009) 76.
- [18] PETIT N., IGNES-MULLOL J., CLARET J. and SAGUES F., *Phys. Rev. Lett.*, **103** (2009) 237802.
- [19] LAZARUS L. L. *et al.*, *ACS Appl. Mater. Interfaces*, **4** (2012) 3077.
- [20] HUANG G. *et al.*, *Talanta*, **100** (2012) 64.
- [21] REZVANTALAB H. and SHOJAEI-ZADEH S., *J. Colloid Interface Sci.*, **400** (2013) 70.
- [22] SHAKERIN S., *Phys. Teach.*, **48** (2010) 316.
- [23] BARR I. A. *et al.*, *Phys. Educ.*, **51** (2016) 043001.
- [24] OTTINO J. M., *The Kinematics of Mixing: Stretching, Chaos, and Transport* (Cambridge University Press, Cambridge) 1989.
- [25] LINKE J., NEUMEYER P., WAECHTER M. and PEINKE J., *Exp. Fluids*, **42** (2007) 811.
- [26] ANDERSEN A. *et al.*, *Phys. Rev. Lett.*, **91** (2003) 104502.
- [27] SERRA M., SATHE P., BERON-VERA F. and HALLER G., *J. Atmos. Sci.*, **74** (2017) 3871.
- [28] VINCZE M. *et al.*, *Met. Z.*, **23** (2015) 611.
- [29] CHURCH C. and BURGERS D., *The Tornado: Its Structure, Dynamics, Prediction, and Hazards* (American Geophysical Union, New York) 1993.
- [30] GREELEY R. *et al.*, *J. Geophys. Res.* **108** (2003) 5041.
- [31] SCHWIESOW R. L. *et al.*, *J. Appl. Met.*, **20** (1981) 341.
- [32] PEDLOSKY J., *Geophysical Fluid Dynamics* (Springer, New York) 1983.